be solved according to the techniques previously outlined. All symbols are defined in the nomenclature.

As a special case consider plane Poiseuille flow, so that the dissipation function $f(y)$ is given by[2]

$$f(y) = (\mu u M^2 16/yw^2)/[(2y/y_w) - 1]^2 \tag{2}$$

For this case, the problem reduces to the solution of the differential equation

$$(\epsilon d^2T/d\xi^2) - \epsilon\tau_w{}^2T - T^4 =$$
$$-\alpha - \beta\tau_w\xi - (8\psi/\tau_w)(2\xi - 1)^2 + (\tau_w\psi/6)(2\xi - 1)^4 \tag{3}$$

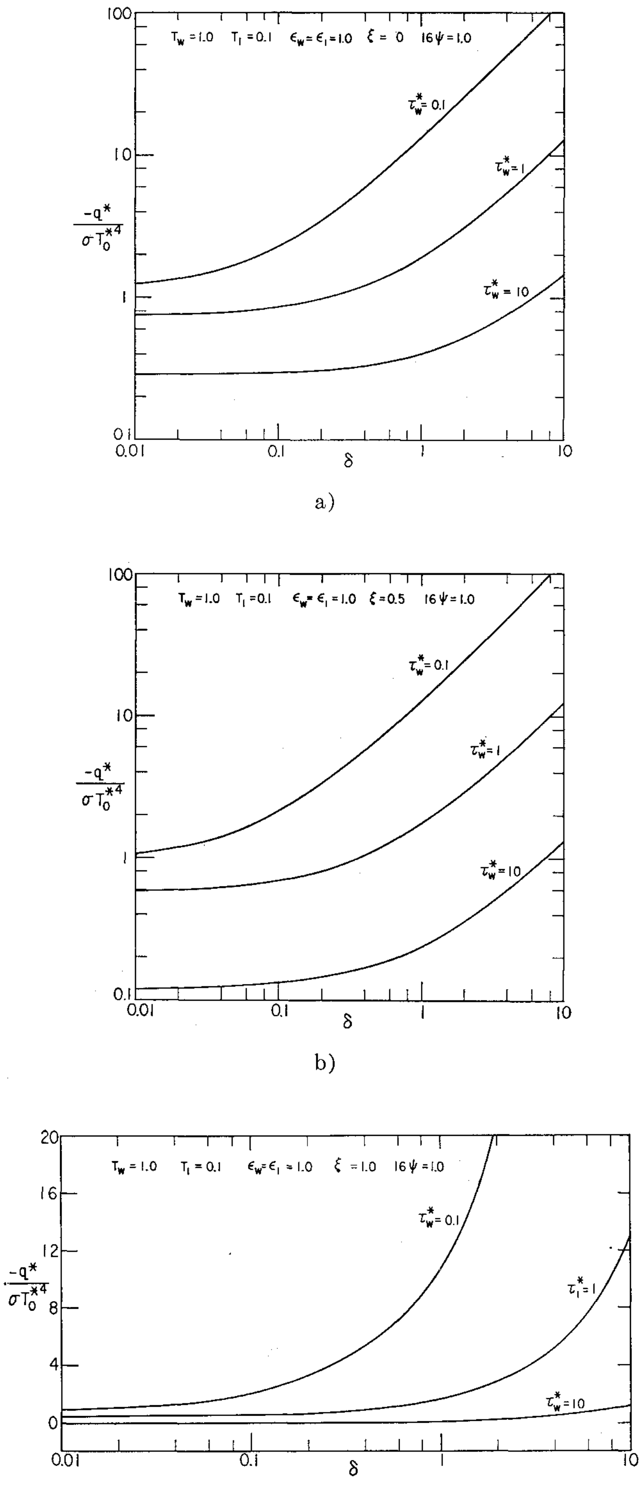

Fig. 1 Heat flux for radiating and conducting Poiseuille flow.

where

$$\alpha = \frac{1}{2 + \tau_w}\left\{ q^-(\tau_w) - q^+(0)[1 + \tau_w] + \delta\left[T_w + T_1(1 + \tau_w) + \left.\frac{dT}{d\tau}\right|_w - \left.\frac{dT}{d\tau}\right|_1 (1 + \tau_w)\right] - \frac{\tau_w\psi}{6}\left[-\tau_w - 10 - \frac{400}{\tau_w} - \frac{384}{\tau_w{}^2} + \frac{384}{\tau_w{}^3} + \frac{384}{\tau_w{}^4}\right]\right\} \tag{4}$$

$$\beta = \frac{1}{2 + \tau_w}\left\{ q^-(\tau_w) - q^+(0) + \delta\left[T_w - T_1 + \left.\frac{dT}{d\tau}\right|_w + \left.\frac{dT}{d\tau}\right|_1\right] - \frac{64\psi}{\tau_w}\left[1 - \frac{1}{\tau_w{}^2}\right]\right\} \tag{5}$$

$$\delta = \epsilon\tau_w{}^2 = \tfrac{3}{4}(\lambda k/\sigma T_0{}^{*3}) \tag{6}$$

$$\psi = \mu u M^2/y_w\sigma T_0{}^{*3} \tag{7}$$

The heat flux is given by

$$-q = 2\beta - 16\psi\ [-\tfrac{1}{6} + \xi - 2\xi^2 + \tfrac{4}{3}\xi^3] \tag{8}$$

Equation (3) may be solved for the following limiting cases: radiation dominant ($\epsilon \ll 1$), conduction dominant ($\epsilon \gg 1$), and for large optical depth ($\tau_w \gg 1$). The results for the heat flux are in good agreement with the radiation slip plus conduction approximation[3]

$$-q = \frac{T_w{}^4 - T_1{}^4}{1 + 3\tau_w{}^*/4} + \frac{(T_w - T_1)}{3\tau_w{}^*/4} - 16\psi\ [-\frac{1}{6} + \xi - 2\xi^2 + \frac{4}{3}\xi^3] \tag{9}$$

The heat flux for plane Poiseuille flow is plotted in Fig. 1 for unequal wall temperatures $T_w = 1$ and $T_1 = 0.1$, for $16\psi = 1$, and for values of ξ equal to 0, 0.5, and 1.

References

[1] Greif, R., "Couette flow of a radiating and conducting gas," AIAA J. **3,** 98–102 (1965).

[2] Schlichting, H., *Boundary Layer Theory* (McGraw-Hill Book Co., Inc., New York, 1955).

[3] Probstein, R., "Radiation slip," AIAA J. 1, 1202–1204 (1963).

Mass-Transfer Cooling of a Flat Plate with Various Transpiring Gases

E. M. Sparrow,* W. J. Minkowycz,† and E. R. G. Eckert‡

University of Minnesota, Minneapolis, Minn.

THE purpose of this note is to provide mass-transfer cooling results for the flat plate, thereby supplementing information for stagnation flows previously published by the authors in Ref. 1. Consideration is given here to a laminar boundary-layer flow into which are injected various gases including hydrogen, helium, water vapor, argon, carbon dioxide, and xenon. The molecular weights of the aforementioned

Received February 23, 1965. The studies described herein were supported by a grant from the U.S. Air Force Office of Scientific Research, Mechanics Division.

* Professor, Department of Mechanical Engineering, Heat Transfer Loboratory.

† Instructor, Department of Mechanical Engineering, Heat Transfer Laboratory.

‡ Professor, Department of Mechanical Engineering, Heat Transfer Laboratory. Associate Fellow Member AIAA.

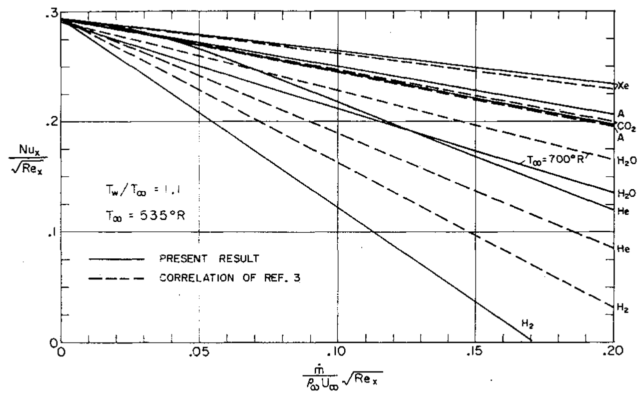

Fig. 1 Flat-plate heat-transfer results, $T_w/T_\infty = 1.1$, $T_\infty = 535°R$.

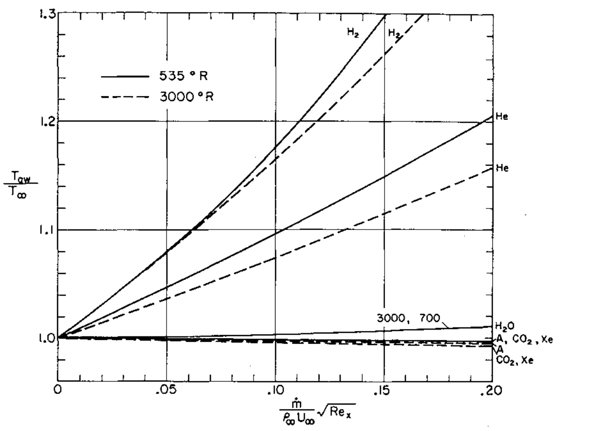

Fig. 3 Adiabatic wall temperature results.

transpiring gases range from 2.016 to 131.3. In all of the cases, the mainstream gas is air (molecular weight = 28.97). The distribution of the surface mass transfer is such that similarity solutions of the boundary-layer equations are possible; that is, the injection velocity v_w varies as $x^{-1/2}$, where x is the distance from the leading edge.

The starting point of the analysis is the conservation equations for mass, momentum, and energy. These are identical to those of Ref. 1, except that the term involving the streamwise pressure gradient is deleted now. In addition to the usual transport terms, the aforementioned conservation equations include heat and mass transfer by mass diffusion, thermal diffusion, and diffusion thermo. The conditions under which the latter pair of processes are significant have been explored previously. Aerodynamic heating has not been included herein.

The thermodynamic and transport properties appearing in the conservation equations are permitted to vary as functions of both temperature and concentration. For all of the injected gases except water vapor, the properties of the pure substances, and the mixtures of these with air, were evaluated as outlined in Ref. 1; a table of the appropriate intermolecular force constants appears in the reference. In the case of water vapor and of water vapor air mixtures, properties were calculated in accordance with very recent information provided by Mason and Monchick.[2]

The partial differential equations of the problem are reduced readily to ordinary differential equations by an appropriate similarity transformation. Inspection reveals that solutions depend upon prescribed values of four parameters: T_w, T_∞, a dimensionless mass injection rate, and the specific transpiring gas. Moreover, the calculations required to achieve solutions are exceedingly lengthy as a consequence of the complex representations of the fluid properties and of the intercoupling of the governing equations. In light of this, consideration has had to be restricted to a few characteristic temperature conditions, and for these, results were obtained for all of the six transpiring gases over a wide range of values of the injection parameter. These heat-transfer results will be compared with the simple correlation rule suggested by Gross and co-workers.[3]

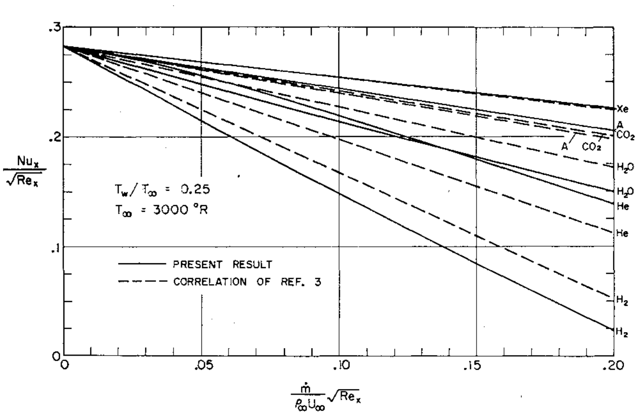

Fig. 2 Flat-plate heat-transfer results, $T_w/T_\infty = 0.25$, $T_\infty = 3000°R$.

Results

The dimensionless parameters employed in the presentation of results will be introduced now. First, the local heat-transfer coefficient h is defined as

$$h = q/(T_w - T_{aw}) \tag{1}$$

in which q is the local rate of heat transfer per unit area, T_w is the wall temperature, and T_{aw} is the adiabatic wall temperature. All of the temperatures are measured in absolute units. In the present investigation, where aerodynamic heating is omitted, the existence of an adiabatic wall temperature differing from the freestream temperature T_∞ is caused entirely by the diffusion-thermo effect. This process is discussed in Ref. 1. The wall heat flux q includes both conductive and diffusional contributions [Eq. (3) of Ref. 1].

The local Nusselt number Nu_x and the local Reynolds number Re_x are based on freestream properties; thus

$$Nu_x = hx/k_\infty \qquad Re_x = U_\infty x/\nu_\infty \tag{2}$$

in which U_∞ denotes the freestream velocity; k_∞ and ν_∞ are the thermal conductivity and the kinematic viscosity of pure air evaluated at T_∞. A dimensionless blowing parameter may be defined as

$$(\dot{m}/\rho_\infty U_\infty)Re_x^{1/2} \tag{3}$$

where $\dot{m}$ is the rate of mass transfer per unit surface area. Inasmuch as $\dot{m} = \rho_w v_w \sim x^{-1/2}$, it is evident that the blowing parameter is independent of position along the plate.

Nusselt number results are presented in Figs. 1 and 2. The first of these pertains to the case $T_w/T_\infty = 1.1$, $T_\infty = 535°R$§; this corresponds to realistic laboratory test conditions. The second figure gives results for the situation $T_w/T_\infty = 0.25$, $T_\infty = 3000°R$, which is suggestive of an aerospace application with a highly cooled wall. In both figures, the quantity $Nu_x(Re_x)^{-1/2}$ is plotted as a function of the dimensionless blowing rate, with the injected gas serving as the curve parameter. The solid lines appearing in the figures correspond to the numerical solutions of the present investigation.

Consideration of Figs. 1 and 2 indicates that the Nusselt number decreases monotonically as the blowing rate increases. With the exception of helium, the forementioned decrease is

§ The T_∞ value for water vapor is selected as 700°R to preclude condensation in the boundary layer.

nearly linear. Further inspection of the figures suggests that the reduction in Nusselt number because of blowing is greater when the molecular weight of the injected gas is lower. However, there are exceptions to this relationship. In particular, in the range of small and moderate blowing rates, the Nusselt numbers corresponding to helium injection lie above those corresponding to water vapor injection. Thus, helium is a less effective coolant, and water vapor is a more effective coolant than might have been expected on the basis of a simple molecular-weight rule. Also, argon and carbon dioxide are somewhat out of order in their effect on Nusselt number, but this is of little practical importance.

The nonlinear variation of the helium results and the interchange of position between the curves for helium and water vapor has been reported previously for stagnation flow.[4] By making comparisons between Figs. 1 and 2, one sees only slight differences in detail; the general trends are identical.

The dashed lines appearing in the figures represent the correlation of Gross and co-workers.[3] The original correlation did not take account of thermal diffusional effects. However, it can be extended to include these effects by replacing q with h; in the correlation equation thus

$$h/h_0 = 1 - [1.82/(C^*)^{1/2}][(M_2/M_1)^{1/3}(\dot{m}/\rho_\infty U_\infty)Re_x{}^{1/2}] \quad (4)$$

where

$$C^* = \rho^*\mu^*/\rho_\infty\mu_\infty \quad (4a)$$

and M_2 and M_1 denote the molecular weights of air and of the injected gas, respectively. It is evident that h_0 represents the heat-transfer coefficient for no mass injection. The quantity C^* is a correction for variable fluid properties; ρ^* and μ^* represent air properties corresponding to a reference temperature T^* that, in the absence of aerodynamic heating, is the average of T_w and T_∞.

It is evident that the correlation equation [Eq. (4)] provides a heat-transfer coefficient that decreases linearly with increasing blowing rate. Furthermore, the correlation predicts a greater decrease in h when the molecular weight is lower.

In view of Figs. 1 and 2, it is clear that the present results are in accord with certain aspects of the correlation equation. However, the correlation does not predict the nonlinear behavior of the helium results. Furthermore, it overpredicts the reduction in heat transfer caused by helium injection and underpredicts the reduction caused by water vapor injection.

The adiabatic wall temperature results calculated as part of the present investigation are presented in Fig. 3. As was noted earlier, the adiabatic wall temperature differs from T_∞ because of the effect of diffusion thermo. Thus, T_{aw} enters the heat-transfer computation through the definition of h [Eq. (1)]. Inspection of Fig. 3 shows that, for injected gases having molecular weights exceeding the mainstream gas (air), $T_{aw}/T_\infty \leq 1$; the opposite is true for injected gases lighter than air. For the very light gases, hydrogen and helium, the difference between T_{aw} and T_∞ becomes substantial at higher blowing rates. On the other hand, for the heavier gases, there is little difference between T_{aw} and T_∞.

References

[1] Sparrow, E. M., Minkowycz, W. J., and Eckert, E. R. G., "Diffusion-thermo effects in stagnation-point flow of air with injection of gases of various molecular weights into the boundary layer," AIAA J. 2, 652–659 (1954).

[2] Mason, E. A. and Monchick, L., "Survey of the equation of state and transport properties of moist gases," *1963 International Symposium on Humidity and Moisture* (National Bureau of Standards, Washington, D. C., May 1963).

[3] Gross, J. F., Hartnett, J. P., Masson, D. J., and Gazley, C., Jr., "A review of binary laminar boundary-layer characteristics," Intern. J. Heat Mass Transfer 3, 198–221 (1961).

[4] Sparrow, E. M., "Recent studies relating to mass transfer cooling," *Proceedings of the 1964 Heat Transfer and Fluid Mechanics Institute* (Stanford University Press, Stanford, Calif., 1964), pp. 1–18.

Effects of Suction and Blowing on Oscillatory Boundary Layers over Cylinders

WEN-JEI YANG*
University of Michigan, Ann Arbor, Mich.

BECAUSE of the importance of the boundary-layer control, there have been extensive studies on the steady, laminar, boundary layer with suction or blowing. Recently, considerable attention has been focused on the oscillatory boundary layers induced by the acoustic waves, vibrations, and flow fluctuations of the periodic-type transients.[1] This paper presents the effects of uniform suction and blowing on the permanent alterations in both the wall shear stress and heat-transfer rate. The alterations are caused by the fluctuations in the magnitude and direction of the freestream velocity, the rotational oscillations of the cylinder surface, the standing waves, and the progressive waves superimposed in an otherwise forced convection field. The analysis is restricted to the quasi-steady state, which may approximate the behaviors of low-frequency fluctuations.

The fundamental equations for unsteady boundary layers have been deduced for two dimensional flow [Ref. 1, Chap. 7, Eqs. (13) and (135)]. Let u and v be the velocity components in the x and y directions, respectively; t, the physical time; x and y, the distances measured along and normal to the cylinder surface, respectively; p, the pressure; T, the fluid temperature; and U, the velocity of potential flow. The boundary conditions are $y = 0$: $u = 0, v = V, T = T_w$; $y = \infty$: $u = U, T = T_\infty$, where V is the velocity of uniform suction for negative value and uniform blowing for positive value; T_w, the temperature of cylinder surface; and T_∞, the fluid temperature of freestream.

Let $U_0(x)$ be the velocity of the potential flow at steady state and $\epsilon U_1 \cos\omega t$ be the periodic disturbance, where

$$U_0(x) = U_\infty \sum_{k=0}^{\infty} a_{2k+1}x^{2k+1}$$

$$U_1(x) = U_\infty \sum_{k=0}^{\infty} b_{2k}x^{2k}$$

ϵU_1, the amplitude of the disturbance; ϵ, a small constant parameter; ω, the circular frequency; and a_{2k+1} and b_{2k} are the coefficients depending upon the geometrical configuration of the cylinder and the nature of disturbance, respectively. If the disturbance is superimposed on the freestream in the form of flow perturbations, then $U(x, t)$ may be expressed as $U_0(x) + \epsilon U_1(x) \cos\omega t$. It is called the flow oscillation for $U_0 = U_1$ and the fluctuating circulation for $U_0 \neq U_1$. Other disturbances, which may be superimposed on the freestream, include standing waves and progressive waves. Two typical cases of standing waves are $\epsilon A \sin(2\pi/\lambda)x \cos\omega t$ for the nodal point of the wave coinciding with the forward stagnation point and $\epsilon A \cos(2\pi/\lambda)x \cos\omega t$ for the point of maximum amplitude coinciding with the forward stagnation point, where ϵA is the magnitude, and λ is the wavelength of the standing waves. By including $A \sin(2\pi/\lambda)x$ or $A \cos(2\pi/\lambda)x$ as $U_1(x)$, the disturbances caused by the standing waves and freestream perturbations may be treated simultaneously. The progressive wave may be expressed as $\epsilon A \sin[(\omega x/U_w) \mp \omega t]$, which represents an infinite train of harmonic waves of frequency ω and amplitude ϵA traveling in the positive or negative direction of x with a velocity U_w. By rewriting in the form of $\epsilon A \sin(\omega x/U_w) \cos\omega t - \epsilon A \cos(\omega x/U_w) \sin\omega t$, the

Received February 8, 1965; revision received April 5, 1965.
* Assistant Professor, Department of Mechanical Engineering.